34th Annual International Conference of the IEEE EMBS
San Diego, California USA, 28 August - 1 September, 2012

Automatic Exudate Detection Using Active Contour Model and Regionwise Classification*

B. Harangi, I. Lazar, A. Hajdu

***Abstract*—Diabetic retinopathy is one the most common cause of blindness in the world. Exudates are among the early signs of this disease, so its proper detection is a very important task to prevent consequent effects. In this paper, we propose a novel approach for exudate detection. First, we identify possible regions containing exudates using grayscale morphology. Then, we apply an active contour based method to minimize the Chan-Vese energy to extract accurate borders of the candidates. To remove those false candidates that have sufficient strong borders to pass the active contour method we use a regionwise classifier. Hence, we extract several shape features for each candidate and let a boosted Naïve Bayes classifier eliminate the false candidates. We considered the publicly available DiaretDB1 color fundus image set for testing, where the proposed method outperformed several state-of-the-art exudate detectors.**

I. Introduction

In the developed countries, diabetic retinopathy (DR) is a prevalent reason of vision loss. More than 360 million people suffered from diabetes in 2011 and this figure is estimated to be 550 million by 2030. That is, the diabetes is a rapidly growing disease that affects large portion of the population. Thus, an automatic screening of DR has growing importance. One of the main tasks of an automatic screening system is to detect DR lesions, such as exudates. This lesion appears on retinal images as bright patches with various size and irregular boundary. In the corresponding literature, a great variety of exudate detection algorithms have been proposed. Some of them based on grayscale morphology [1-3] and others on pixel based classification [4-6]. In this paper, we attempt to merge the advantages of these approaches within a single framework. As an extension we use a regionwise classification instead of the pixel-level one.

As for the steps of the proposed approach, first we apply a morphology-based method for candidate extraction. This step emphasizes almost all bright regions in the image. To improve sensitivity, we use an active contour method (ACM) which determines the correct boundary of the candidates. The applied ACM considers sparse field method to minimize the well-known Chan-Vese energy function [8]. After the determination of the correct boundaries, we extract several shape descriptors for all regions in order to classify them as true or false exudates candidates. For this task we use Naïve Bayes classifier with an adaptive boosting technique to enhance its performance.

The rest of the paper is organized as follows: in section 2, we give a short description of the applied image preprocessing steps and candidate extraction using morphological operators. Section 3 is devoted to determining the correct boundaries of the candidates via active contours. In section 4, we explain the details of feature extraction and the Naïve-Bayes classifier which is optimized by an adaptive boosting method. Then, in section 5, we present our experimental results and finally some conclusions are drawn in section 6.

II. Preprocessing and Candidate Selection

Exudates appear as bright, yellowish pattern on color fundus images. Their shape and size vary in a wide range and their boundaries are also quite irregular. These variations in their properties cause difficulty in automatic exudate detection.

A. Elimination of the Optic Disc

The primary problem is the high order similarity in appearance between the optic disc (OD) and exudates. Hence, the first common task is the elimination of the OD. In our former work [9], we proposed an ensemble of algorithms based on different principles benefiting from their strength and compensating their weaknesses for localization of the OD. Based on the combined results of optic disc detectors we exclude the OD region from the procedure of exudate detection.

B. Image preprocessing

The RGB color fundus images have three intensity channels: red, green and blue. The green channel (G) contains most of information about lesions and the anatomical parts of the retina. Hence, we perform our proposed method on this channel. Moreover, to enhance the local contrast of exudates we apply contrast-limited adaptive histogram equalization (CLAHE) to the green channel (G_{Clahe}). This image processing technique can improve the local contrast of the image so the edges of the exudates are enhanced. Besides CLAHE, we consider another contrast improvement technique ($G_{imadjust}$) which maps the intensity values such that 1% of data is saturated at low and high intensities of the green channel.

C. Candidate Extraction

In this section, we present how we extract the regions which possibly contain exudates. These extracted regions will be used as initial positions for the active contour segmentation method.

* This work was supported in part by the TECH08-2 project DRSCREEN – Developing a computer based image processing system for diabetic retinopathy screening of the National Office for Research and Technology of Hungary (contract no.: OM-00194/2008, OM-00195/2008, OM-00196/2008), by OTKA/NK101680 - Mathematical modeling of clinical observations for improved melanoma detection and by the TÁMOP-4.2.2/B-10/1-2010-0024 project which is co-financed by the European Union and the European Social Fund.

B. Harangi, I. Lazar, A. Hajdu are with the University of Debrecen, Faculty of Informatics, Debrecen, 4010 POB. 12, Hungary (e-mail: {harangi.balazs,lazar.istvan,hajdu.andras}@inf.unideb.hu).

Walter et al. proposed a morphology based technique [1] for the detection of exudates, which has relative high precision. In order to localize exudate regions, it considers the high local contrast and high intensity values of $G_{imadjust}$. Since, there is also high contrast between the vessels and the background, the method needs to eliminate the vascular system by a simple grayscale morphological closing with properly adjusted structure element. On this vessel-free image, the local variation is calculated at each pixel within a window. To obtain regions of bright objects, an adjusted thresholding is applied. To refine the region of a candidate, morphological reconstruction is used and the result is subtracted from $G_{imadjust}$. The drawback of this method is that it finds almost all bright, yellowish patches on the retinal image and the boundaries of the detected exudates are not precise either. Moreover, in some cases mainly at retinal images of young patients, it marks the shine, longish regions which spread along the temporal arcade as exudates. For these reasons we consider this approach as candidate detector and go on with consequent steps for more precise detection.

III. Active Contour Model

Our aim besides the recognition of the existence of each possible exudate on the retinal image is the proper description of their exact shape. We try to retain their correct boundary and size to improve the accuracy of our proposed method. For this reason, we apply an active contour model which can determine the most likely boundary of an extracted candidate. The result of the candidate extraction step is a binary image and whose boundary is used as an initial position for the active contour model as illustrated in Figure 1.

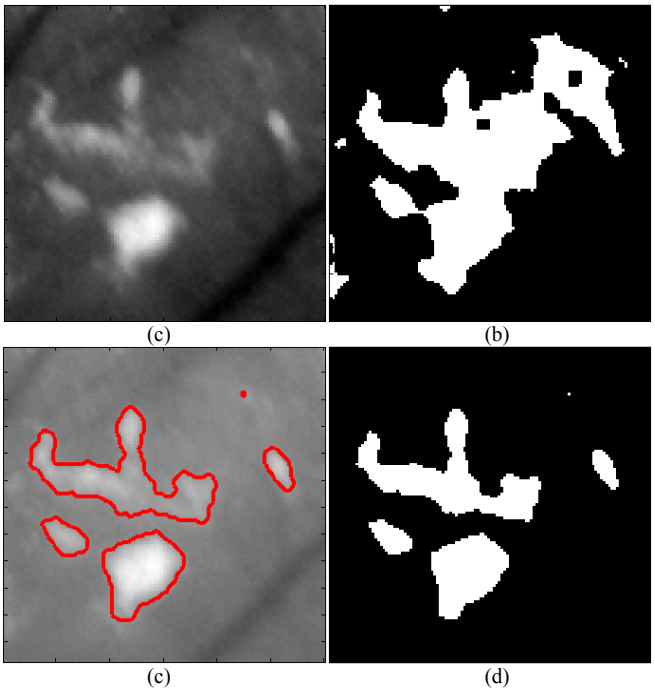

Figure 1. (a) Green channel of a part of a fundus image. (b) Result of the candidate extractor for the initialization of the active contour. (c) Result of the active contour method. (d) The final regions with a more precise shape information.

An active contour method can allow the contour to vary iteratively so that it can divide the image into separate regions. A corresponding regular level set method is proposed in [10]. It allows complex boundary behavior, but requires heavy computations via the solution of partial differential equations. As an alternate solution to reduce the processing time significantly, we considered the sparse field method (SFM) proposed by Whitaker [11].

SFM does not require the solution of partial differential equations; it works with lists of points corresponding to the pixel level sets. In this way, points can be very efficiently inserted/removed to/from the proper lists according the distance from the zero level set. One limitation of SFM is that the segmentation energy function is evaluated only along the zero level set, so new curves cannot appear spontaneously.

In our scenario, the initial zero level set is generated from the result of the candidate extraction step. The SFM takes each candidate region separately and the initial zero level set consists of its boundary pixels. To determine the zero level set to the next iteration, the SFM minimizes the well-known Chan-Vese energy function (1). The advantage of this energy function is that it is capable to segment an exudate that has smoother boundaries. The evaluation of the curve depends only on the difference of pixel intensities ($I_{x,y}$) and average intensities inside (c_1) and outside (c_2) the curve (C) as formulated in (2).

$$E_{Chan\_Vese} = F_1(C) + F_2(C), \tag{1}$$

$$F_1(C) = \int_{inside(C)} |I_{x,y} - c_1|^2 \, dxdy,$$
$$F_2(C) = \int_{outside(C)} |I_{x,y} - c_2|^2 \, dxdy. \tag{2}$$

With applying the SFM level set method and Chan-Vese energy function, we can extract the exudates with high precision considering their boundary as shown in Figure 2.

IV. Classification of Segmented Regions

As we mentioned in Section 2, image enhancement is considered as preprocessing to increase the number of positive candidates. However, this step also enhances

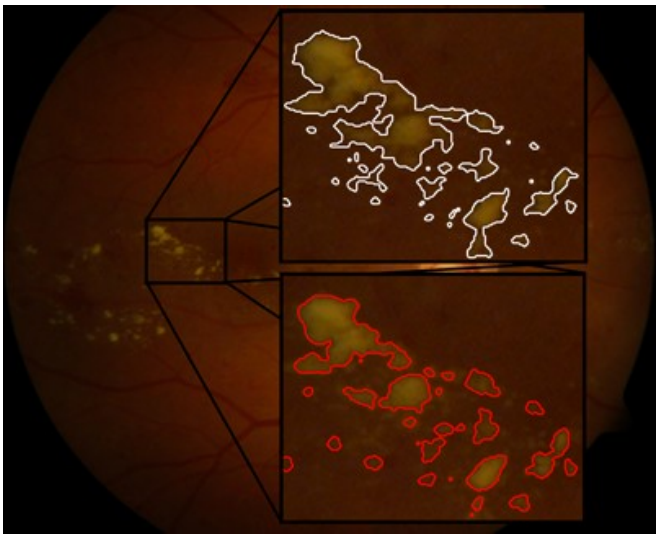

Figure 2. White boundary marks the result of the candidate extractor while red shows the result of the SFM.

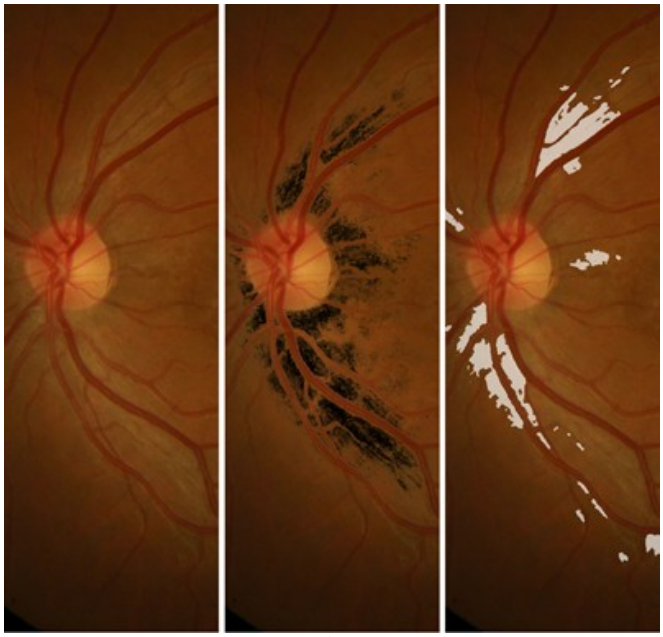

(a) (b) (c)

Figure 3. (a) Retinal image of a young person. (b) The region which causes many false positiv is marked by black. (c) False exudate regions are white.

negative candidates as well, like regions close to vessels or on retinal images of young persons (see Figure 3). That is, we further try to separate the output regions of the SFM as true or false exudates. For this classification we propose a post-processing step which is based on regionwise classification.

A. Feature Extraction and Selection

For feature selection, we have divided the publicly available DiaretDB1 dataset [12] into a training and a test part and we have executed the algorithms described in II.A, II.B, II.C and III. steps on the training images. A medical expert manually labeled the output regions as true or false ones. To find efficient features for classification, we calculated several shape and statistical descriptors (approximately 50) for these segmented regions and selected the most useful ones with applying a two-sample *t*-test for each of them.

Initially, as a pool for selecting the features, we have examined the following descriptors of the candidates: mean, standard deviation (STD), range (difference of minimal and maximal), minimal and maximal value of the gradients under the selected region and under the boundary of the region; the mean, standard deviation, range, minimal and maximal value of the intensities under the region and under the boundary of them on the G, G_{Clahe} and $G_{imadjust}$ images; the compactness of the regions defined as (3); and finally the cardinalities of the region.

$$compactness = perimeter^{1.5}/area. \quad (3)$$

We have also observed that the spatially large false positive regions usually contain some tiny holes. Since exudates often appear close to the center of the image (macula-centered case), we calculated the distance between the candidate regions and the anatomical parts like the optic disc, macula and thick vessels. We also determined the angles of the line connecting the center of the optic disc and the regions.

To coarsely detect the thick vessels, we apply morphological closing with structuring elements of different sizes, and we calculated their differences [13]. For macula detection, we considered our former work [9].

Most of these descriptors are appropriate to differentiate true exudate candidates from false ones. However, several descriptors values have weaker classification performance. These less relevant descriptors cause inaccurate labeling in the classification. Thus, we select only the relevant descriptors with two-sample t-tests. First, we standardize each extracted descriptor individually. Then, we execute the *t*-test by calculating

$$t_j = \frac{(\mu_{j_F} - \mu_{j_T}) \cdot \sqrt{\frac{n \cdot m \cdot (n+m-2)}{n+m}}}{\sqrt{(n-1) \cdot {\sigma_{j_F}}^2 + (m-1) \cdot {\sigma_{j_T}}^2}}, \quad (4)$$

for the jth descriptor where, n is the number of the true exudate regions and m is the number of false ones in the training database. μ_{j_T} ($/\mu_{j_F}$) denotes the mean and σ_{j_T} ($/\sigma_{j_F}$) denotes the standard deviation of the jth descriptor from the training database of all true (/false) regions.

Based on the t_j values, we can rank the descriptors regarding their information content. Overall, we selected the first 18 descriptors (see Table 1) as the optimal set of features for classification.

TABLE I. THE ORDER OF THE FEATURES ACCORDING TO THE *t*-TEST VALUES.

No.	Feature	No.	Feature	No.	Feature
1.	number of holes	7.	mean gradient under the border	13.	max of gradient under the border
2.	size of the region	8.	range of G_{Clahe} under the border	14.	range of G under the region
3.	angle of the line	9.	min gradient under the border	15.	max of gradient under the region
4.	distance from macula	10.	compactness of the shape	16.	distance from the optic disc
5.	STD of G under the region	11.	distance from thick vessel	17.	range of G_{Clahe} under the region
6.	mean gradient under the region	12.	STD of G under the border	18.	max of G under the region

B. Classification

The performance of the considered Naïve Bayes (NB) classifier is rather limited because the method assumes independent feature model while in the practice the features usually depend on each other. To improve the accuracy of the classifier and the detection of exudates we apply the adaptive boosting (AdaBoost) technique [14] to optimize the NB classifier. The basic idea of the AdaBoost is that the performance of the ensemble learning is usually significantly better than that of single learning. Hence, the performance of the boosted NB may be higher than a simple Support Vector Machine (SVM) or *k*-Nearest Neighbors (kNN). However, AdaBoost works well only with a weak learner because the created model can be less dispose to overfit.

V. RESULTS

We have evaluated the performance of our proposed method on the DiaretDB1 dataset [12] which contains 89 color fundus images. We have divided this database into a training and a test part containing 28 and 61 images.

To be able to quantitatively compare the performance of our algorithm with other state-of-the-art exudate detectors, medical experts marked the exudates on this dataset. As evaluation, we consider the *F*-Score (5) to measure the performance. The *F*-Score can be interpreted as a weighted average of the sensitivity (6) and the positive predictive value (PPV) (7). The number of the true positive (TP), false positive (FP) and false negative (FN) are considered at pixel level.

$$F\text{–Score} = \frac{2 \cdot Sensitivity \cdot PPV}{Sensitivity + PPV}, \quad (5)$$

$$Sensitivity = \frac{TP}{TP + FN}, \quad (6)$$

$$PPV = \frac{TP}{TP + FP}. \quad (7)$$

Table II contains the accuracy of the implemented state-of-the-art algorithms in the comparison regarding their *F*-Score on test part of the DiaretDB1 dataset. For the sake of completeness, we also describe the sensitivity and PPV.

TABLE II. COMPERATIVE RESULTS FOR THE PROPOSED METHOD.

	***F*-Score**	**Sensitivity**	**PPV**
Proposed method	**0.75**	0.75	0.75
Walter [1]	0.67	0.76	0.59
Sopharak [2]	0.56	0.40	0.91
Welfer [3]	0.31	0.19	0.92
Jaafar [7]	0.17	0.89	0.09
Sopharak [4]	0.16	0.49	0.09
Sopharak [5]	0.11	0.82	0.06
Sánchez [6]	0.15	0.38	0.10

As we can see from the table, our proposed algorithm outperformed the investigated ones [1-7] regarding the *F*-Score. Figure 4 also presents an example for the output of our proposed algorithm.

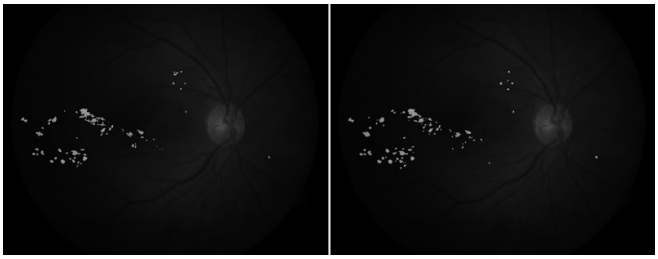

(a) (b)

Figure 4. (a) Result of manual segmentation. (b) Result of the proposed method.

VI. CONCLUSION

In this paper, we have proposed an exudate detection algorithm which merges morphological operators, active contour method and regionwise classification. To improve the sensitivity of the morphology-based step, we retain the rather irregular boundary of the exudates by using an active contour model. For this objective, we applied sparse field algorithm as a level set method to minimize the Chan-Vese energy function. Some of the extracted regions are not true exudates, so we further applied regionwise classification. For this step, we extracted specific descriptors for each candidate region and evaluated their efficiency. Then, we have ranked the descriptors based on the result of *t*-tests, and selected the most efficient 18 ones as features. For classification, we have applied the Naïve-Bayes classifier which is optimized by an adaptive boosting technique. Our experimental results showed that the proposed method outperformed several state-of-the-art approaches.

REFERENCES

[1] T. Walter, J. C. Klein, P. Massin and A. Erginay, "A contribution of image processing to the diagnosis of diabetic retinopathy – detection of exudates in color fundus images of the human retina", *IEEE Transactions on Medical Imaging*, vol. 21, no. 10, pp. 1236–43, 2002.

[2] A. Sopharak, B. Uyyanonvara S. Barman and T. H. Williamson, "Automatic detection of diabetic retinopathy exudates from non-dilated retinal images using mathematical morphology methods", *Computerized Medical Imaging and Graphics*, vol. 32, no. 8, pp. 720–727, 2008.

[3] D. Welfer, J. Scharcanski and D. R. Marinho, "A coarse-to-fine strategy for automatically detecting exudates in color eye fundus images", *Computerized Medical Imaging and Graphics*, vol. 34, no. 3, pp. 228–235, 2010.

[4] A. Sopharak, B. Uyyanonvara and S. Barman, "Automatic exudate detection from nondilated diabetic retinopathy retinal images using fuzzy c-means clustering", *Sensors*, vol. 9, no. 3, pp. 2148–2161, 2009.

[5] A. Sopharak, M. N. Dailey, B. Uyyanonvara, S. Barman, T. Williamson, K. T. Nwe and Y. A. Moe, "Machine learning approach to automatic exudate detection in retinal images from diabetic patients", *Journal of Modern Optics*, vol. 57, no. 2, pp. 124-135, 2010.

[6] C. I. Sánchez, R. Hornero, M. I. López, M. Aboy, J. Poza and D. Abásolo, "A novel automatic image processing algorithm for detection of hard exudates based on retinal image analysis", *Medical Engineering & Physics*, vol. 30, no. 3, pp. 350-357, 2008.

[7] H. F. Jaafar, A. K. Nandi and W. Al-Nuaimy, "Detection of exudates in retinal images using a pure splitting technique", *Engineering in Medicine and Biology Society* (EMBC 2010), pp. 6745-6748, 2010.

[8] T. Chan, and L. Vese, "Active Contours Without Edges". *IEEE Transactions on In Image Processing*, vol. 10, no. 2, pp. 266-277, 2001.

[9] R. J. Qureshi, L. Kovacs, B. Harangi, B. Nagy, T. Peto, A. Hajdu, "Combining algorithms for automatic detection of optic disc and macula in fundus images", *Computer Vision and Image Understanding*, vol. 116, no. 1, pp. 138-145, 2012.

[10] J. A. Sethian, "Level Set Methods and Fast Marching Methods: Evolving Interfaces in Computational Geometry, Fluid Mechanics, Computer Vision, and Materials Science" 2nd ed., Cambridge University Press, 1999.

[11] R. T. Whitaker, "A Level-Set approach to 3D reconstruction from range data," *International Journal of Computer Vision*, vol. 29, no. 3, pp. 203-231, 1998.

[12] T. Kauppi, V. Kalesnykiene, J. K. Kmrinen, L. Lensu, I. Sorri, A. Raninen, R. Voutilainen, H. Uusitalo, H. Klviinen, and J. Pietil, "Diaretdb1 diabetic retinopathy database and evaluation protocol", *Medical Image Understanding and Analysis* (MIUA 2007), pp. 61-65, 2007.

[13] S. Ravishankar, A. Jain, A. Mittal, "Automated Feature Extraction for Early Detection of Diabetic Retinopathy in Fundus Images", *IEEE Conference on Computer Vision and Pattern Recognition* (CVPR 2009), pp. 210-217, 2009.

[14] R. Polikar, "Ensemble based system in decision making", *IEEE Circuits and Systems Magazine*, vol. 6, no. 3, pp. 21-45, 2006.